

Unlearning regularization for Boltzmann Machines

Enrico Ventura,^{1,2} Simona Cocco,² Rémi Monasson,² and Francesco Zamponi^{1,2}

¹*Dipartimento di Fisica, Sapienza Università di Roma, P.le A. Moro 2, 00185 Roma, Italy*

²*Laboratoire de Physique de l'École Normale Supérieure, ENS, Université PSL, F-75005 Paris, France*

Boltzmann Machines (BMs) are graphical models with interconnected binary units, employed for the unsupervised modeling of data distributions. As all models, in absence of a proper regularization BMs may over-fit the training data and thus provide a poor estimate of the distribution that generated them. In this study, we introduce a regularization method for BMs to improve generalization by reducing the susceptibility of the model under rescaling of the parameters. The new technique shares formal similarities with the unlearning algorithm, an iterative procedure used to improve memory associativity in Hopfield-like neural networks. We test our unlearning regularization on synthetic data generated by two simple models, the Curie-Weiss ferromagnetic model and the Sherrington-Kirkpatrick spin glass model, and we show that it outperforms L_p -norm schemes. Finally, we discuss the role of parameter initialization.

I. INTRODUCTION

Boltzmann Machines (BMs) [1–3] are a class of graphical models, capable of modelling data distributions through the learning of effective pairwise interactions between variables. Once properly trained *e.g.* through gradient ascent of the likelihood, BMs can be used to generate new data configurations, which hopefully are indistinguishable from the ones in the dataset [4]. Good generative performances are, in practice, hindered by the limited availability of training data, possibility leading to the overfitting phenomenon. Informally speaking, overfitting is an over-specialization of the model, which is too focused on the details of the specific training set, rather than capturing the broader statistical structure highlighted by the data.

Overfitting is particularly concerning in the so-called high dimensional setting, in which the size of the model (the dimension of the data configuration) is comparable to the amount of available data. In this regime, regularization can be used to help the model generalizing, *i.e.* performing well on test data. Standard schemes for regularization include L_2 - and L_1 -norm penalties imposed on the pairwise interactions. However, these regularization schemes have a tendency to decrease the values of the interactions, and introduce systematic biases in the model. In a statistical physics language, the inferred interactions are smaller than their ground-truth counterpart (formally obtained with infinite data), and the inferred model is implicitly at higher temperature. Correct this bias requires introducing a temperature parameter smaller than unity when generating new data. This procedure was used in Ref. [5] to generate new viable protein sequences with BMs inferred from evolutionary sequence data. However, this approach is purely empirical and somewhat uncontrolled. It is known from the statistical physics literature that rescaling the energy function by a temperature factor, even close to one, can drastically alter the distribution properties if the system is near a phase transition point [6, 7].

The goal of this study is to propose a new regulariza-

tion technique for BM learning that explicitly aims at increasing the robustness of the model under rescaling of its parameters, *i.e.* the coupling matrix $\mathbf{J} = \{J_{ij}\}$ and the local fields $\mathbf{h} = \{h_i\}$. This new tool, that we named unlearning regularization, appears to be more effective than other techniques, approaching a better generalization performance of the neural network. The performance of the unlearning regularization is evaluated from artificial data generated by both a Curie-Weiss (CW) and a Sherrington-Kirkpatrick (SK) models with a small number of variables. In this way the original parameters are known, the fixed points of the learning equations are reached precisely and the useful quantities can be computed exactly.

A particular limit of this type of regularization coincides with a thermal version of the traditional Hebbian Unlearning algorithm (HU) [8–11]. We hence evaluate this particular case of study and conclude that HU is able to infer the original data distribution with a very good degree of generalization. The performance shows an optimum in time that scales with the control parameters, as it has been observed when the algorithm is implemented in associative memory tasks [12]. We conclude that HU can be interpreted as a two-steps BM learning procedure.

The structure of the article is the following. We first introduce generative modeling and Boltzmann Machines in section II. Some extensively employed regularization techniques (*i.e.* the L_p methods) are then described in section II B. Section III briefly describes the Hebbian Unlearning algorithm and its traditional use in associative memory models. The new unlearning regularization is then defined in section IV and its generalization performance is analyzed for two different data sources: a CW model (section IV A) and a SK model (section IV B). In section V we compare the new regularization method to the standard L_p regularization method, showing that it improves generalization substantially. The study of a particular limit of the regularization technique leading to HU follows in section VI, which provides some insight on its behavior as a generic inference tool.

II. GENERATIVE MODELING

Generative models are a class of specific neural networks that are able to learn the probability distribution of a data-set and generate brand new data that exhibit maximum coherence with the same statistics [3, 4]. Imagine to have a collection of N variables in a vector $\vec{S} = (S_1, \dots, S_N)$. Data are M realizations of such a vector grouped into a set $\{\vec{S}^\mu\}_{\mu=1}^M$ and sampled independently from a joint distribution $P_{true}(\vec{S})$. Given M data, we have access to the frequency of occurrence of a certain variable, i.e. the empirical distribution

$$P_{data}(\vec{S}) = \frac{1}{M} \sum_{\mu=1}^M \prod_{i=1}^N \delta_{S_i^\mu, S_i}. \quad (1)$$

Generative modeling looks for a model distribution $P_{mod}(\vec{S}|\hat{\theta})$, where the parameters $\hat{\theta}$ are inferred from the training data such that P_{mod} is the closest possible to P_{data} . However, P_{data} might still differ from the ground-truth distribution P_{true} . As a remedy, it is useful to reduce the number of degrees of freedom of the problem by designing the model depending on some hints that we have about P_{true} . For instance one might choose a *graphical model*, where variables are sketched as the nodes of a graph [3] with interactions to be inferred, rather than setting a prior distribution for the variables as a *mixture of Gaussians* of unknown means and unit variances [13]. *Regularization* techniques are used for this purpose, i.e. to reduce the number of parameters, and thus allowing P_{mod} to get closer to P_{true} . The generative approach is largely implemented across several disciplines such as computational neuroscience [14, 15], bio-informatics [16], animal behaviour [17], physical simulations [18], image and text synthesis [19–21].

A. Boltzmann Machines

We now describe a specific graphical model of generative neural networks, which will be particularly relevant to the present work. It is inspired by equilibrium statistical mechanics and it is called Boltzmann Machine (BM) [1–3, 22].

Consider a fully connected network of binary N Ising variables $\vec{S} \in \{-1, +1\}^N$ with the following energy function

$$E[\vec{S}|\mathbf{J}, \mathbf{h}] = - \sum_{i,j>i}^{1,N} S_i J_{ij} S_j - \sum_{i=1}^N h_i S_i, \quad (2)$$

where J_{ij} are symmetric couplings and h_i are the fields acting on each neuron site. We know, from statistical mechanics, that such a system at equilibrium at a temperature β^{-1} obeys the following *Gibbs-Boltzmann* joint probability distribution

$$P_{mod}(\vec{S}|\mathbf{J}, \mathbf{h}, \beta) = \frac{1}{Z_\beta} \exp\left(-\beta E[\vec{S}|\mathbf{J}, \mathbf{h}]\right), \quad (3)$$

with

$$Z_\beta = \sum_{\vec{S}} \exp\left(-\beta E[\vec{S}|\mathbf{J}, \mathbf{h}]\right), \quad (4)$$

where β can be set to one without any effect in the training. Training a Boltzmann Machine means finding the parameters \mathbf{J} and \mathbf{h} that minimize the distance between P_{data} given by Eq. (1) and P_{mod} given by Eq. (3). This can be achieved by minimizing the Kullback-Leibler divergence between P_{data} and P_{mod} , i.e.

$$\mathcal{L}(\mathbf{J}, \mathbf{h}) = - \sum_{\vec{S}} P_{data}(\vec{S}) \log\left(\frac{P_{mod}(\vec{S}|\mathbf{J}, \mathbf{h})}{P_{data}(\vec{S})}\right), \quad (5)$$

which is equivalent to maximizing the cross-entropy of P_{mod} with respect to the empirical distribution P_{data} . Differentiating eq. (5) with respect to J_{ij} and h_i , we obtain the gradient of the loss, i.e.

$$\nabla_{ij} \mathcal{L} = \langle S_i S_j \rangle_{mod} - \langle S_i S_j \rangle_{data}, \quad (6)$$

$$\nabla_i \mathcal{L} = \langle S_i \rangle_{mod} - \langle S_i \rangle_{data}, \quad (7)$$

where $\langle \cdot \rangle_{data}$ and $\langle \cdot \rangle_{mod}$ are the averages over the respective probability distributions. Therefore, the parameters can be found by iterating the following gradient descent equations

$$\delta J_{ij} = -\lambda \nabla_{ij} \mathcal{L} = \lambda (\langle S_i S_j \rangle_{data} - \langle S_i S_j \rangle_{mod}), \quad (8)$$

$$\delta h_i = -\lambda \nabla_i \mathcal{L} = \lambda (\langle S_i \rangle_{data} - \langle S_i \rangle_{mod}), \quad (9)$$

with λ being a small positive learning rate.

Note that the mean and covariance over the data can be computed upstream, because they only depend on the training data-set; on the other hand, the moments of P_{mod} must be re-sampled at each step of the training process, because their exact calculation would involve a sum over all possible \vec{S} . Sampling can be performed by a sufficient number of Monte Carlo chains at equilibrium at $\beta = 1$, which requires an algorithm time that is long enough to ensure ergodicity for each chain. Usually the number of chains should be of the same order of magnitude of M , the number of training data-points, in order for the corrections to the empirical averages not to be sub-dominant with respect to the sampled ones.

Once the process converges to the fixed points of Eq. (8) and Eq. (9) we obtain a *moment matching* condition, i.e. the first and the second moments of the two probability distributions coincide. While, in principle, the training of a BM is a convex problem that admits a unique solution [2], in practice there are many flat directions such that some initial conditions can push the parameters closer to their optimal configuration. A good choice is, for instance

$$J_{ij}^{(0)} = \langle S_i S_j \rangle_{data} - \langle S_i \rangle_{data} \langle S_j \rangle_{data}, \quad (10)$$

and

$$h_i^{(0)} = \text{atanh}(\langle S_i \rangle_{data}), \quad (11)$$

because Eq. (10) and Eq. (11) are generally close to the fixed point of Eqs. (8) and (9).

In order to measure the quality of the training of a BM one can measure whether the moment matching condition is met or not. The observable to measure in this case is the Pearson coefficient between the moments of the P_{mod} and P_{data} distributions at the end of the training. Let us collect the two-points correlation matrices $\langle S_i S_j \rangle$ in a vector \vec{c} where each entry runs over the indices $i, j > i$. Let us group the means $\langle S_i \rangle$ in a similar vector $\vec{\mu}$ where each entry runs over the index i . Then the Pearson coefficients will be defined as

$$\rho_J = \frac{\sum_i c_i^{mod} c_i^{data}}{\sqrt{\sum_i (c_i^{mod})^2} \sqrt{\sum_i (c_i^{data})^2}}, \quad (12)$$

$$\rho_h = \frac{\sum_i \mu_i^{mod} \mu_i^{data}}{\sqrt{\sum_i (\mu_i^{mod})^2} \sqrt{\sum_i (\mu_i^{data})^2}}. \quad (13)$$

B. Regularization in Boltzmann Machines

L_p regularizations are certainly the most famous regularization methods, also due to their intuitive interpretation. This approach penalises high values of the parameters by adding a L_p norm of the same variables in the expression of the loss function. As a consequence, the sparsity of the graph is promoted: the redundant parameters are weakened with respect to the relevant ones. The expression of the loss of a BM with L_1 and L_2 regularizations is given by the following equations

$$\mathcal{L}_1 = \mathcal{L}^{BM}(\mathbf{J}, \mathbf{h}) + \gamma_1 \sum_{i,j>i} |J_{ij}| + \gamma_1 \sum_i |h_i|, \quad (14)$$

$$\mathcal{L}_2 = \mathcal{L}^{BM}(\mathbf{J}, \mathbf{h}) + \frac{\gamma_2}{2} \sum_{i,j>i} J_{ij}^2 + \frac{\gamma_2}{2} \sum_i h_i^2, \quad (15)$$

where \mathcal{L}^{BM} is defined in Eq. (5) and γ_1, γ_2 are two small regularization rates. This translates into new updating rules for the parameters, i.e.

$$\delta J_{ij}^{(1)} = \delta J_{ij}^{BM} - \lambda \gamma_1 \text{sign}(J_{ij}), \quad (16)$$

$$\delta h_i^{(1)} = \delta h_i^{BM} - \lambda \gamma_1 \text{sign}(h_i),$$

$$\delta J_{ij}^{(2)} = \delta J_{ij}^{BM} - \lambda \gamma_2 J_{ij}, \quad (17)$$

$$\delta h_i^{(2)} = \delta h_i^{BM} - \lambda \gamma_2 h_i.$$

We are now interested in a criterion that describes the generalization performance of a BM. Let us divide generalization into two features: one feature corresponds to the similarity of P_{mod} to P_{true} , in terms of a measure in the space of the probability distributions; the second feature corresponds to the robustness of the network to small variations of the parameters.

The first aspect can be quantified by the Kullback-Leibler divergence $D_{KL}(true|mod)$ between the inferred model and the original one, defined as

$$D_{KL}(true|mod) = \sum_{\vec{S}} P_{true}(\vec{S}) \log \left(\frac{P_{true}(\vec{S})}{P_{mod}(\vec{S})} \right). \quad (18)$$

This quantity is not symmetric under the exchange of the two distributions, which can be inconvenient to define a distance. We can then adopt a symmetric version of the divergence as

$$sD_{KL}(true, mod) = D_{KL}(true|mod) + D_{KL}(mod|true). \quad (19)$$

Even if numerical results do not show a significant difference between these two quantities, we will mainly adopt sD_{KL} in our analysis.

Regarding the second trait, it is known that Ising-like models inferred via BM learning are close to be critical [6, 7, 23]. Criticality is associated with a susceptibility of the system to small variations of the temperature and can be measured through the *specific heat* [24], defined as

$$C_v(\beta) = -\beta \frac{\partial S_\beta}{\partial \beta} = \beta^2 (\langle E^2 \rangle_\beta - \langle E \rangle_\beta^2), \quad (20)$$

where S_β is the entropy of the model at a given inverse temperature β . The fact that inferred neural networks typically display a peak in C_v around the value of β used for training implies the vicinity of a critical point (the finite size of the system impedes C_v to properly diverge and to show a real criticality). Therefore, since all parameters naturally scale with β in Eq. (3), C_v is a measure of the sensitivity of the model to a small perturbation of the parameters: high values of C_v imply a strong variation of the model entropy with a small variation of the parameters, which suggests strong variations of the inferred statistics as well. The study of Ref. [25] concludes that a large peak in C_v derives from over-fitting, since there is a strong correlation between the increase in generalization due to regularization, and a significant lowering of the peak. Intuitively, a model that generalizes well should be robust to small changes in the parameters, and it should thus display small values of C_v .

III. UNLEARNING ALGORITHM

Inspired by the brain functioning during REM sleep [26], the Hebbian Unlearning algorithm (HU) [8–10, 26–29] is a training procedure for simple associative models.

Consider a neural network having the same energy defined in Eq. (2). We assume the external local fields to be null, i.e. $h_i = 0, \forall i$. The associative memory task consists in retrieving a set of random neural states $\{\vec{\xi}^\mu\}_{\mu=1}^{\alpha N}$, called *patterns*, through a zero temperature Monte Carlo dynamics initialized on some corrupted versions of them. The control parameter α is the *capacity* of the model. Associativity is improved by achieving larger basins of attraction of the patterns.

The training procedure starts by initializing the connectivity matrix in the Hebb's fashion as in Eq. (10), i.e. $J_{ij}^0 = \langle S_i S_j \rangle_{data}, \forall i, j$, where $\langle \cdot \rangle_{data}$ is the empirical average over the patterns. Then, the following routine is iterated at each step t :

1. Initialize the network on a random neural state.
2. Run the asynchronous dynamics until convergence to a stable fixed point \vec{S}^* .
3. Update couplings according to:

$$\delta J_{ij}^{(t)} = -\frac{\lambda}{N} S_i^* S_j^*, \quad J_{ii} = 0 \quad \forall i. \quad (21)$$

This algorithm was first introduced in Ref. [8] to prune the landscape of attractors from proliferating spurious states, i.e. fixed points of the neural dynamics not coinciding with the patterns [30, 31]. This pruning action stabilizes the patterns and increases the size of the basins of attraction. The numerical analysis of Ref. [10] shows that HU approaches the memory performance of a maximally stable symmetric perceptron, which is considered to be a very effective model, up to a critical capacity $\alpha_c \simeq 0.6$. Another important aspect to underline is that HU performs at its best at a given amount of algorithmic iterations that scales with N, α and λ [9, 10]. After this amount of steps the performance of the model, in terms of perfect retrieval of the patterns and size of the basins of attraction, deteriorates. This implies the necessity of applying an *early-stopping* criterion for the HU algorithm to perform optimally. We also note that HU is an *unsupervised* algorithm, in the sense that it does not need to be provided explicitly with the patterns, and only exploits the information encoded in Hebbian initialization of the couplings.

IV. UNLEARNING REGULARIZATION

We now propose a new type of regularization that has the objective of imposing the maximum robustness under rescaling of the parameters, i.e.

$$\mathbf{J} \longrightarrow a\mathbf{J}, \quad \mathbf{h} \longrightarrow a\mathbf{h}, \quad \text{with } a \geq 0. \quad (22)$$

We can interpret this operation as a redefinition of the inverse temperature β in the inferred model. We will evaluate the performance of this method on different types of data-sets, and we will compare it to L_p regularization

schemes, showing a gain in the generalization capability of the network.

For the model to be robust under a redefinition of the parameters, we can minimize the mutual distance between two models at different temperatures, say $\beta = 1$ and $\beta = a$, as well as the distance between one of these two models and the training data. Hence, let us define the following loss function

$$\mathcal{L}(\mathbf{J}, \mathbf{h}|a) = D_{KL}(a|data) + D_{KL}(1|a), \quad (23)$$

with

$$D_{KL}(a|data) = \sum_{\vec{S}} P_{data}(\vec{S}) \log \left(\frac{P_{data}(\vec{S})}{P_a(\vec{S})} \right), \quad (24)$$

and

$$D_{KL}(1|a) = \sum_{\vec{S}} P_a(\vec{S}) \log \left(\frac{P_a(\vec{S})}{P_1(\vec{S})} \right), \quad (25)$$

being the Kullback-Leibler divergences between the data and the model P_a , and that between the two models P_1 and P_a , respectively. Notice we use here the asymmetric KL distance; the reason for this choice will be evident in a few lines. The gradient descent equations for this loss function become

$$\delta J_{ij} = \lambda [a (\langle S_i S_j \rangle_{data} - \langle S_i S_j \rangle_a) - (\langle S_i S_j \rangle_1 - \langle S_i S_j \rangle_a)], \quad (26)$$

$$\delta h_i = \lambda [a (\langle S_i \rangle_{data} - \langle S_i \rangle_a) - (\langle S_i \rangle_1 - \langle S_i \rangle_a)]. \quad (27)$$

When $a = 1$, Eqs. (26) and (27) coincide with the original BM learning. In the limit $a \rightarrow 0$ one has $\langle S_i S_j \rangle_{a=0} \rightarrow 0$ and Eq. (26) tends to a thermal version of the HU rule performed at $\beta = 1$, i.e.

$$\delta J_{ij} = -\lambda \langle S_i S_j \rangle_1,$$

which is similar to previous attempts in the associative memory literature [12]. On the other hand, when $a \rightarrow \infty$, and the learning rate is redefined as $\lambda = \tilde{\lambda}/a \rightarrow 0$, the algorithm becomes

$$\delta J_{ij} = \tilde{\lambda} (\langle S_i S_j \rangle_{data} - \langle S_i S_j \rangle_\infty),$$

which also resembles the unlearning procedure: the sampling at $a = \infty$ produces fixed points of the zero-temperature dynamics, which gives back Eq. (21). At variance with the standard routine, there is an additional Hebbian *homeostatic* term $\langle S_i S_j \rangle_{data}$ which impedes the couplings to vanish at convergence.

At this point, the motivation for our choice of the loss function $\mathcal{L}(\mathbf{J}, \mathbf{h}|a)$ should be clear: we search for an algorithm that interpolates between the BM learning algorithm and HU. In this way HU emerges as a particular limit of a regularization method on BMs.

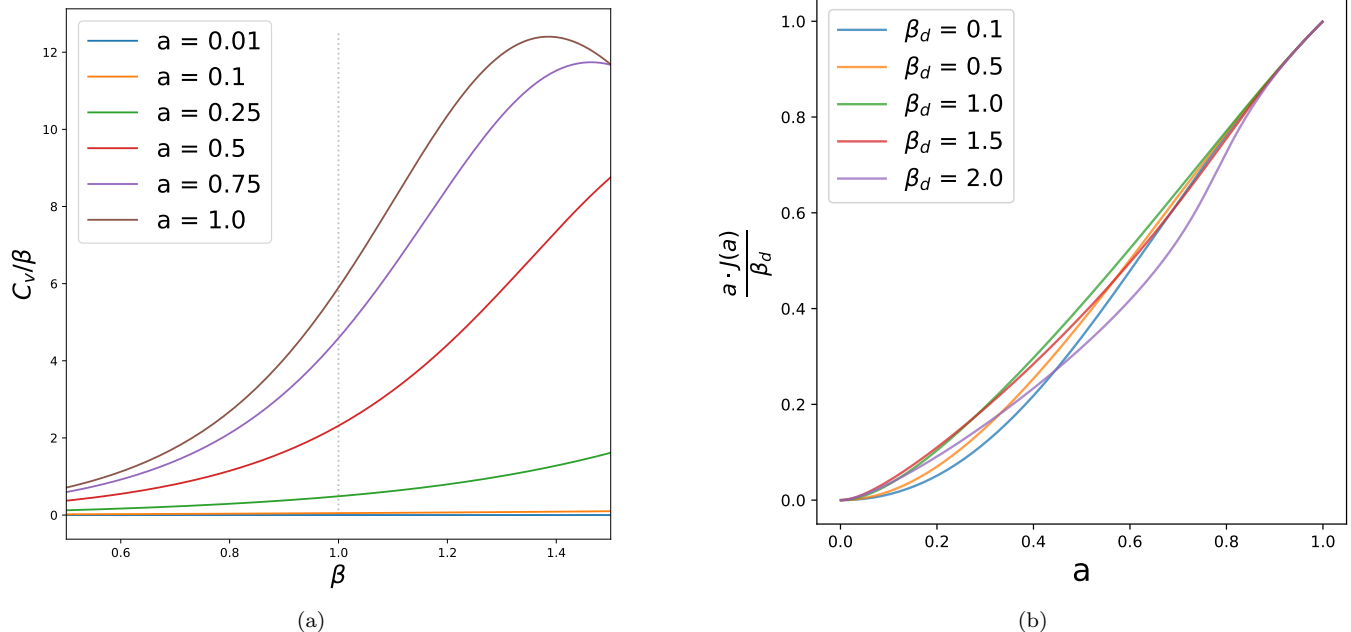


FIG. 1. Inferred couplings and specific heat for a small network trained on data generated by a CW model with $N = 20$ spins and given β_d . (a) The specific heat of the inferred model for $\beta_d = 1$ is reported as a function of the model temperature β , at different values of the regularization parameter a . (b) Inferred couplings multiplied by a/β_d as a function of a at different values of β_d : the linear regime displays the robustness of the parameters under rescaling.

For the rest of our study we consider a small sized network, i.e. $N \sim 18 \div 20$, which allows us to consider the limit of infinite number of generated data, i.e. $M \rightarrow \infty$. In this limit, we can reach the fixed points of Eqs. (26) and (27) precisely, whenever such points are admitted, with no errors due to the finite sampling. We can then compute the observables C_v or sD_{KL} more easily, in order to determine the generalization performance of the system. For simplicity of notation we rename

$$\langle S_i S_j \rangle_{data} = c_{ij}^d, \quad \langle S_i S_j \rangle_{\beta} = c_{ij}^{\beta},$$

where we will mainly deal with $\beta = a$ and $\beta = 1$. The inverse temperature of the data generating model is $\beta = \beta_d$. For given β_d , we can compute c_{ij}^d exactly in the limit $M \rightarrow \infty$ by exact enumeration of the model configurations. The generating models for the data will be of two kinds: a mean field fully connected ferromagnetic Ising network (i.e. the Curie-Weiss model) and a fully disordered spin glass network (i.e. Sherrington-Kirkpatrick [32]), which both display a critical point in the thermodynamic limit, manifested by a singularity of the specific heat at a given critical temperature. This singularity is smoothed in finite size systems, thus appearing as a peak in specific heat. In our small systems, solving the BM learning equations leads to the exact parameters of the generating model. Instead, solving Eqs. (26) and (27) leads to a non-trivial network with its own generalization capability.

A. Curie-Weiss model

We first consider the problem of inferring a Curie-Weiss model (CW), that is defined by the following energy function

$$E_{CW}[\vec{S}|\mathbf{J}] = - \sum_{i,j>i} S_i J_{ij} S_j, \quad J_{ij} = \frac{J}{N}, \forall i, j. \quad (28)$$

This model can be treated fully analytically in the finite size case, and the solution procedure for the main quantities is here reported. Since fields are zero, by construction of the model, we are interested in the evolution equation for the couplings, i.e.

$$\dot{J} = \lambda [a(c_d - c_a(t)) - (c_1(t) - c_a(t))], \quad (29)$$

where we used the fact that both couplings and correlation functions assume the same values $\forall i, j$. The parameters are initialised as $J^{(0)} = c_d$ and $h^{(0)} = 0$. Notice that all elements of the matrices are identical, because each node receives the same fields from its neighbours. The fixed point equation for the correlation functions from Eq. (29) is

$$c_a^* = \frac{c_1^*}{1-a} - \frac{a}{1-a} c_d, \quad (30)$$

where the star indicates the value of the correlations at convergence. Moreover we know that

$$Z_{\beta J} = \sum_m \binom{N}{\frac{N}{2}(1+m)} \exp\left(\frac{\beta J}{2}(Nm^2 - 1)\right), \quad (31)$$

where $m \in [-1, -1 + \frac{1}{N}, \dots, 1 - \frac{1}{N}, +1]$ and we used

$$E_{CW}[\vec{S}|J] = -J \left[N \left(\frac{1}{N} \sum_i S_i \right)^2 - 1 \right] \quad (32)$$

$$= -J(Nm^2 - 1).$$

Moreover, the second moment of the magnetization with respect to the Gibbs-Boltzmann measure $\langle m^2 \rangle_\beta$ can be written as

$$I_N(\beta J) = \frac{\sum_m m^2 \binom{N}{\frac{N}{2}(1+m)} \exp \frac{\beta}{2} J(Nm^2 - 1)}{\sum_m \binom{N}{\frac{N}{2}(1+m)} \exp \frac{\beta}{2} J(Nm^2 - 1)} = \frac{1 + (N-1)c(\beta J)}{N}. \quad (33)$$

Thus

$$c(\beta J) = \frac{NI_N(\beta J) - 1}{N - 1}. \quad (34)$$

Eq. (30) becomes

$$c(aJ) = \frac{c(J)}{1-a} - \frac{a}{1-a} c(\beta_d J), \quad (35)$$

or equivalently

$$I_N(aJ) = \frac{I_N(J)}{1-a} - \frac{a}{1-a} I_N(\beta_d J), \quad (36)$$

that has to be solved for J , given a and β_d .

In the following, we first choose $\beta_d = 1$ in order to generate data from the paramagnetic phase of a network of $N = 20$ spins slightly above the critical point, since the specific heat peak of the model at $N = 20$ appears to be at $\beta > 1$. Then, we solve Eq. (36) to obtain the coupling $J(a)$ of the inferred model in presence of the unlearning regularization. Once this is done, we analyze the resulting model by computing quantities from the Gibbs-Boltzmann distribution with parameter $\beta J(a)$ rescaled by an additional temperature β . Results are reported in fig. 1a and show that the specific heat has a peak slightly after $\beta = 1$ that flattens progressively when a is decreased. Next, in fig. 1b we compute $J(a)$ for different values of β_d and plot the quantity $aJ(a)/\beta_d$ as a function of a . The lines are approximately linear, signaling that $J(a)$ is nearly constant in a . The inferred model thus changes slowly upon varying a .

B. Sherrington-Kirkpatrick model

Next, we consider the problem of inferring a Sherrington-Kirkpatrick model (SK), i.e.

$$E_{SK}[\vec{S}|J] = - \sum_{i,j>i} S_i J_{ij} S_j, \quad J_{ij} \sim \mathcal{N}(0, N^{-1/2}). \quad (37)$$

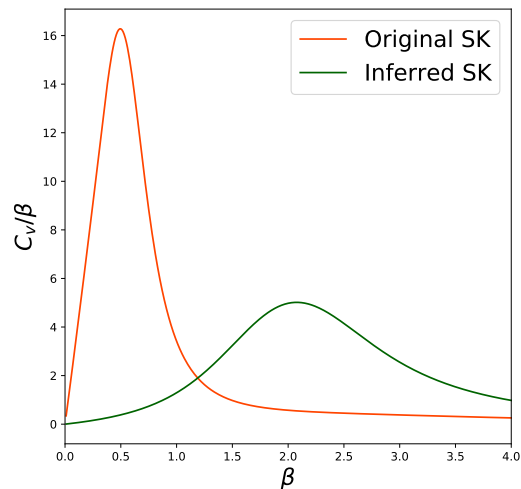


FIG. 2. Specific heat C_v/β as a function of the inverse temperature β for the single SK spin-glass used in our study, and for the inferred model with the unlearning regularization. Choice of the parameters: $N = 18$, $a = 0.3$, $\beta_d = 0.4$, $\lambda = 0.06$.

We consider a network of $N = 18$ spins with a data generation temperature $\beta_d = 0.4$. For clarity of the results, we will use only one realisation of the parameters for the SK, having a peak in the specific heat at a β slightly larger than β_d , as represented in fig. 2. The parameters are initialised as $J_{ij}(0) = c_{ij}^d$ and $h_i(0) = 0 \forall i$.

We compare the specific heat C_v/β of the original model with that of the model obtained through inference with the unlearning regularization, at convergence of the update Eq. (8), with the choice of $a = 0.3$. We want to stress that the inference procedure gives us the matrix $\mathbf{J}(a)$ associated to the particular choice of a , and the specific heat at each β is then computed from a Gibbs-Boltzmann distribution with parameters $\beta \mathbf{J}(a)$. The results displayed in fig. 2 show that the inferred system has a lower peak, that is also shifted towards higher values of β , as observed in the CW case.

Figure 3 shows the Pearson coefficient ρ for the two-point correlation matrices c_a, c_1 and the sD_{KL} between the inferred model with $\beta = a$ and $\beta = 1$ and the original SK model, both as functions of the algorithm steps and the parameter a . As one can conclude from fig. 3a and fig. 3b, the quality of the correlation between c_d and c_β is better for $\beta = 1$ with respect to $\beta = a$. This is probably due to the fact that the gradient deriving from $D_{KL}(a|data)$ in Eq. (26) is weighted through the parameter a , that in our setting is smaller than unity. The same trend is observed with sD_{KL} in fig. 3c and fig. 3d: the model with $\beta = 1$ approaches the original system way more closely than the one with $\beta = a$ at any value of a . We conclude that the unlearning regularization is able to reproduce the statistics of the original model at $\beta = \beta_d$, and reaches a higher robustness under variation of the parameters, which makes it a good generative model.

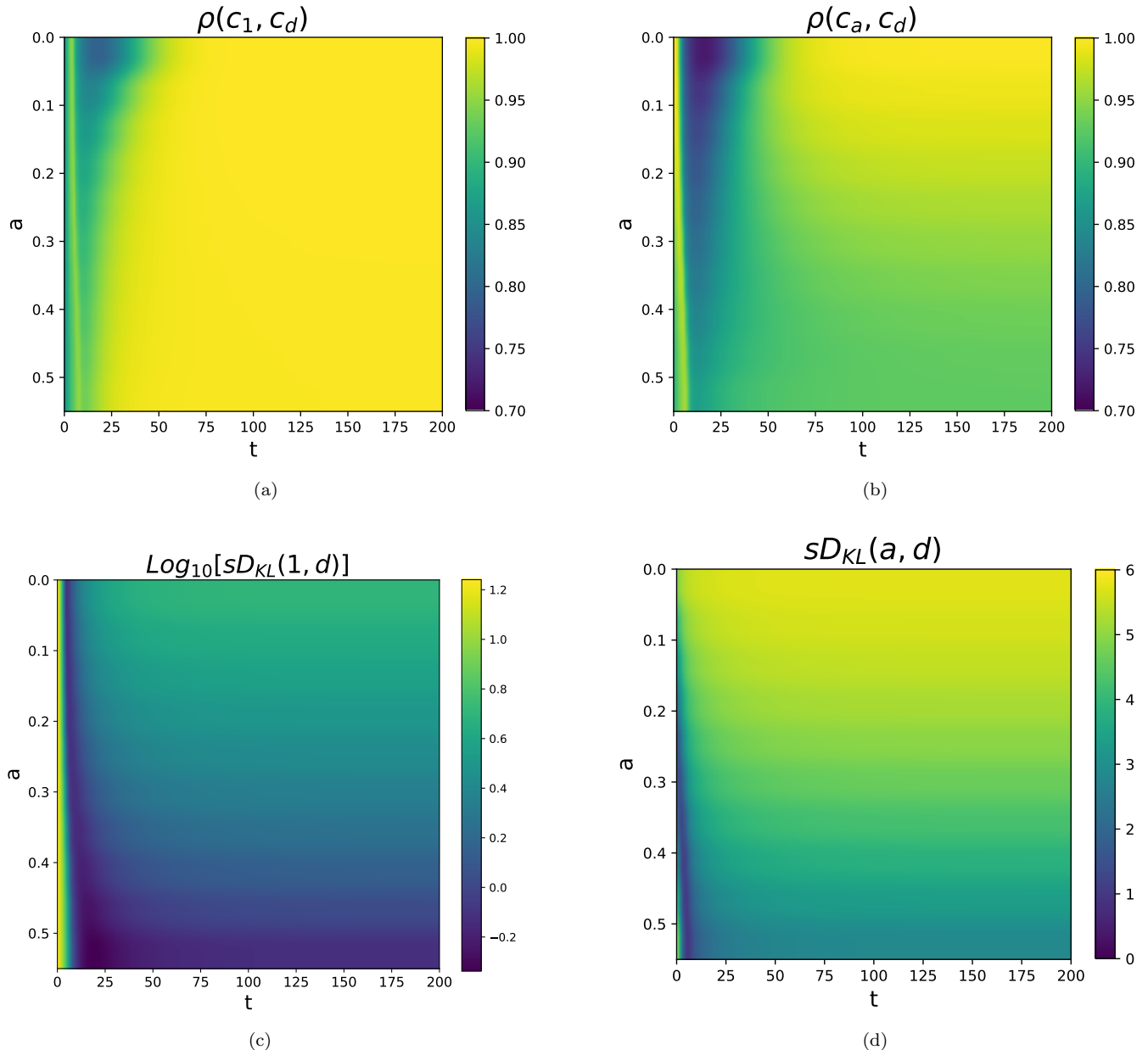


FIG. 3. Relevant observables for the inference of a small SK model, as functions of the regularization parameter a and the algorithmic time t . The generating model for the data has inverse temperature $\beta_d = 0.4$. Parameters are initialized in the standard way, i.e. $\mathbf{J}^{(0)} = c_d$ and $\mathbf{h}^{(0)} = 0$. $\rho(A, B)$ is the Pearson coefficient between the elements of the matrices A and B , while $sD_{KL}(\beta, d)$ is the symmetrized Kullback-Leibler divergence between the Gibbs-Boltzmann distribution at β and the original one that generated the data. Choice of the parameters: $N = 18$, $\lambda = 0.06$.

C. Initialization of the parameters

As one can notice from fig. 3, both ρ and sD_{KL} show a transient regime in the first few training steps. In this interval, ρ oscillates while the sD_{KL} reaches its minimum value, pushing the model to its best generalizing configuration of the parameters. This holds for both the models with $\beta = a$ and $\beta = 1$. Fig. 4 shows results for a model regularized via the unlearning scheme with $a = 0.3$ and

compares the standard Hebbian initialization of the couplings with other two types of initializations: $J_{ij}^{(0)} = 0$ and $J_{ij}^{(0)} \sim \mathcal{N}(0, N^{-1/2}) \forall i, j$. The study is repeated for both $\beta = 1$ and $\beta = a$, showing a general better performance when $\beta = 1$, as was observed from fig. 3. Since the transient regime does not appear in the other two initializations, we conclude that the initialization of couplings plays a fundamental role in the training of a BM.

For the sake of completeness, we underline that the

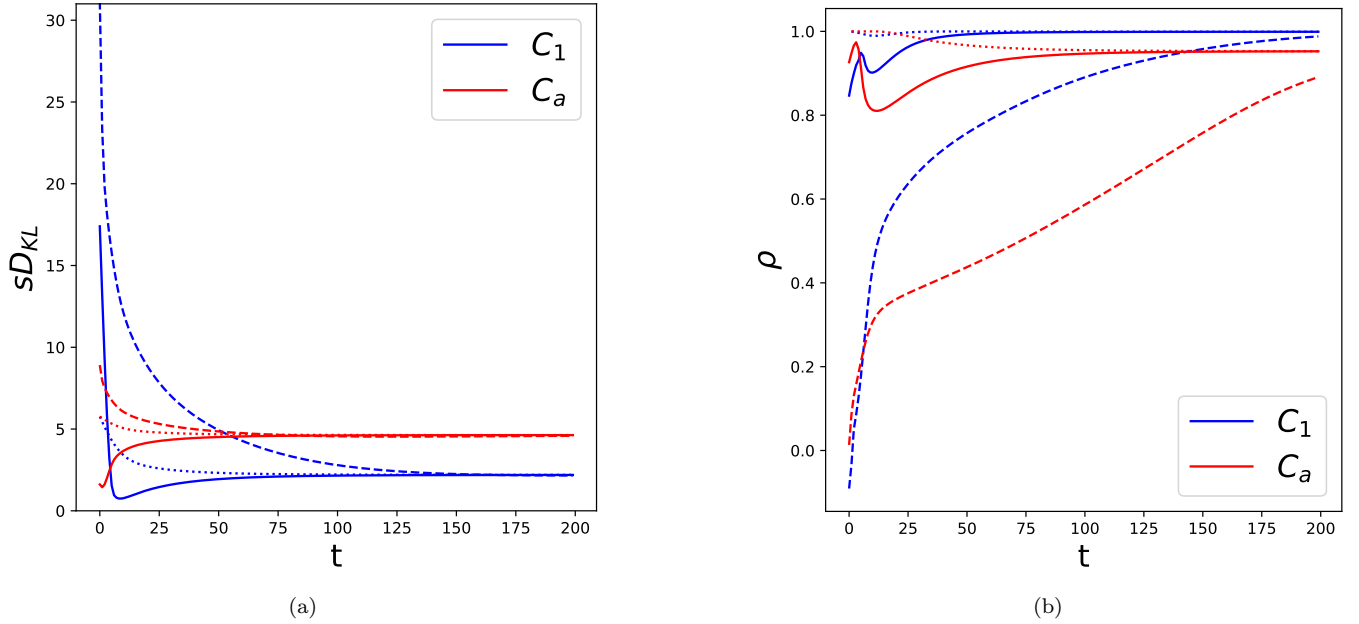


FIG. 4. (a) Pearson coefficient ρ between the correlation matrix c_β with $\beta = a$ and $\beta = 1$ and the data correlation matrix c_d as a function of time t . (b) Symmetric Kullback-Leibler divergence, as a function of time t , between the inferred Gibbs-Boltzmann distribution at $\beta = a$ and $\beta = 1$ and the one describing a SK model at $\beta_d = 0.4$. The *full* line reports the case of Hebbian initialization of the couplings; the *dashed* line corresponds to a random initialization; the *dotted* line represents the initialization to $\mathbf{J}^{(0)} = 0$. Choice of the parameters: $N = 18$, $a = 0.3$, $\lambda = 0.06$.

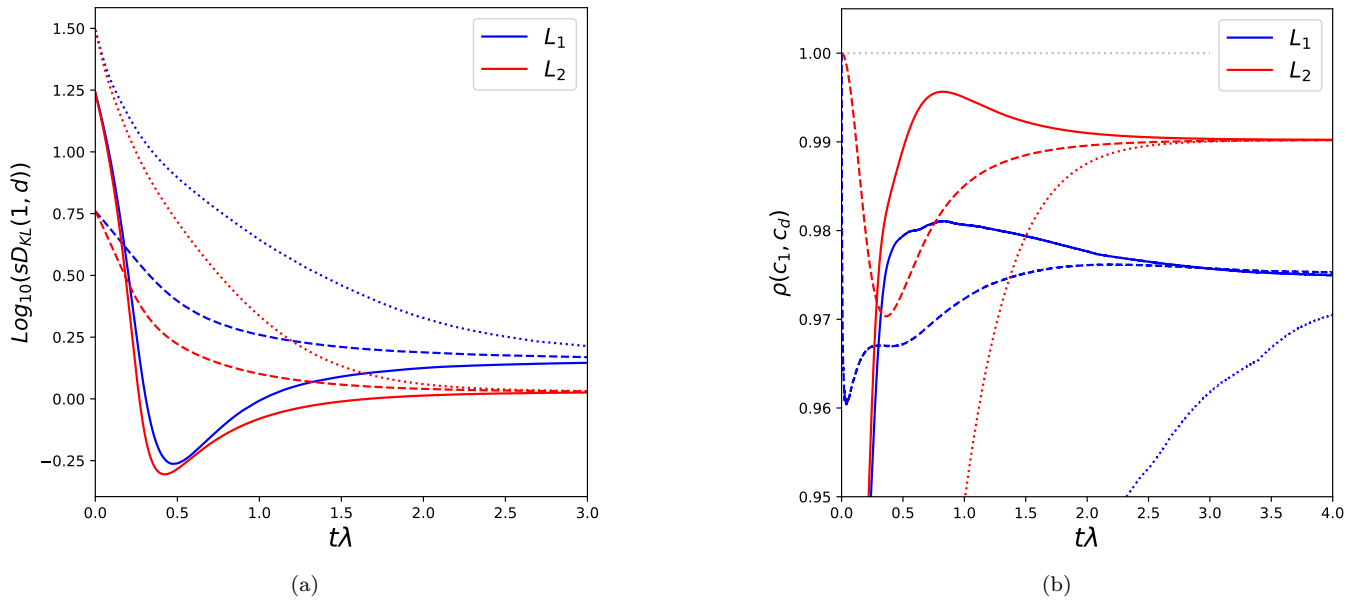


FIG. 5. (a) Symmetric Kullback-Leibler divergence in log-scale between the generating model and the inferred one at unitary temperature via L_1 and L_2 regularizations, as a function of the normalized time $t\lambda$. (b) Pearson coefficient between the elements of the empirical correlation matrix c_d and the two point correlations at unitary temperature c_1 , as a function of the normalized time $t\lambda$. *Continuous* lines reports the Hebbian initialization, *dotted* lines represent random initializations and *dashed* lines show the case of null initial couplings. Choice of the parameters: $N = 18$, $\beta_d = 0.4$, $\lambda_1 = \lambda_2 = 0.001$, $\gamma_1 = 0.15$, $\gamma_2 = 1$.

same behavior of ρ and sD_{KL} is measured when other types of regularizations are employed in the training. We

specifically consider a BM regularized via the L_1 and L_2 methods, i.e. trained according to Eqs. (16) and (17)

on the same data generating model. Figure 5 reports the evolution in time of the $sD_{KL}(1, d)$ and the Pearson coefficient ρ between the elements of the empirical data correlation matrix c_d and the thermal correlations of the model c_1 at unitary temperature. One can notice the existence of a double regime when parameters are initialized in the Hebbian fashion: a peak in ρ coincides with a minimum reached by sD_{KL} after a certain amount of algorithm iterations. Our analysis suggests that early-stopping might be required to reach the best generalization performance when using L_p regularizations. A heuristic explanation of this double regime behaviour, based on the study of the training dynamics in BMs, will be proposed in section VI.

V. COMPARING DIFFERENT REGULARIZATION TECHNIQUES

It is now necessary to compare the generalization performance of the unlearning method with other kinds of regularization. We will consider, in particular the L_1 and L_2 types described in section II B. Data are always generated from a SK model with $\beta_d = 0.4$, as in section IV B.

The couplings are optimized until convergence of the learning algorithm for the three types of regularizations. Three quantities are measured after training: the symmetric Kullback-Leibler divergence $sD_{KL}(1, d)$ between the model at unitary temperature and the original SK model, the specific heat at unitary temperature $C_v(1)$ and the standard deviation of the couplings σ_J . Measures are repeated for different choices of the regularization parameters $\{a, \gamma_1, \gamma_2\}$ in order to obtain a range of σ_J that is sufficiently large. The results are reported in fig. 6. Specifically, fig. 6a is a colour plot showing the performance of the network in the plane $(sD_{KL}, C_v(1))$, where each point is coloured according to the standard deviation σ_J . The origin $(0, 0)$ of this diagram is associated to the best possible generalization performance. Nevertheless we know that this limit cannot be reached with a non-zero σ_J , since the model that generates the data has non-zero $C_v(1)$, by construction. The plots shows three lines relative to the three regularizations: the unlearning line is generally closer to the origin than the L_1 and L_2 ones, suggesting a higher generalization performance. To better compare the three methods, fig. 6b reports the distance of the points reported in fig. 6a from the origin directly as a function of the standard deviation σ_J . It is, in fact, crucial to compare the outcomes from the three techniques at equal values of σ_J . The plots shows that the set of points relative to unlearning stands always below the L_1 and L_2 ones, corroborating the previous observations. Different experiments with different data and temperatures β_d show very similar results.

Moreover, the U and L_2 curves reproduce the same trend when σ_J is vanishing, i.e. when all inferred couplings are small. This can be explained through a weak coupling expansion of the gradient equations for U and

L_2 . When $\sigma_J \ll 1$ the two-point correlation functions can be Taylor expanded as

$$c_{ij}^\beta(t) = \beta J_{ij}^{(t)} + \mathcal{O}(J_{ij}^{(t)2}). \quad (38)$$

The expansion of Eq. (26) leads to

$$\delta J^{(t)} = \lambda \left(ac_d - (1-a)J^{(t)} + \mathcal{O}(a^2) \right). \quad (39)$$

Since σ_J is small when $a \ll 1$, in this limit we obtain

$$\delta J^{(t)} \simeq ac_d - J^{(t)}, \quad (40)$$

which at the fixed point becomes

$$J = ac_d \longrightarrow \sigma_J = a\sigma_d, \quad (41)$$

where σ_d is the standard deviation of the empirical correlation matrix. By repeating the same procedure with Eq. (17) one obtains

$$\delta J^{(t)} = \lambda \left(c_d + (1-\gamma_2)J^{(t)} \right), \quad (42)$$

which at the fixed point becomes

$$J = \frac{c_d}{\gamma_2 - 1} \longrightarrow \sigma_J = \frac{\sigma_d}{\gamma_2 - 1}, \quad (43)$$

for $\gamma_2 > 1$, which is justified by the fact that σ_J is small when γ_2 is sufficiently large. Numerics support the fact that, when $\sigma_J \ll 1$ and σ_J is the same in fig. 6 for both U and L_2 , then $a(\gamma_2 - 1) = 1$. Our results show that the HU algorithm, achievable from the unlearning regularization when $a \rightarrow 0$, can be reproduced by a L_2 type regularization with a large γ_2 .

Furthermore, fig. 7 plots the profiles of the specific heat C_v/β as a function of the inverse temperature β of the original SK model and the three regularization methods for a comparison. Specifically, we choose three values of σ_J that are associated to the local minima of the curves in fig. 6b, namely the best performances for each regularization method. The plot shows that the peaks for the regularized networks are lower and shifted to the right, with respect to the original SK model, but the profile for L_2 is generally higher than the unlearning one, which is in turn higher than the L_1 one. This hierarchy is conserved across the three choices of σ_J . At variance with the previous analysis that appeared robust from experiment to experiment, the behavior of the specific heat may change with β_d .

VI. THE HEBBIAN UNLEARNING LIMIT

We will now study the specific limit of the unlearning regularization that leads to an algorithm which strongly resembles the HU routine. The inferential performance of the learning procedure is examined by measuring the distance between the inferred model and the original one at

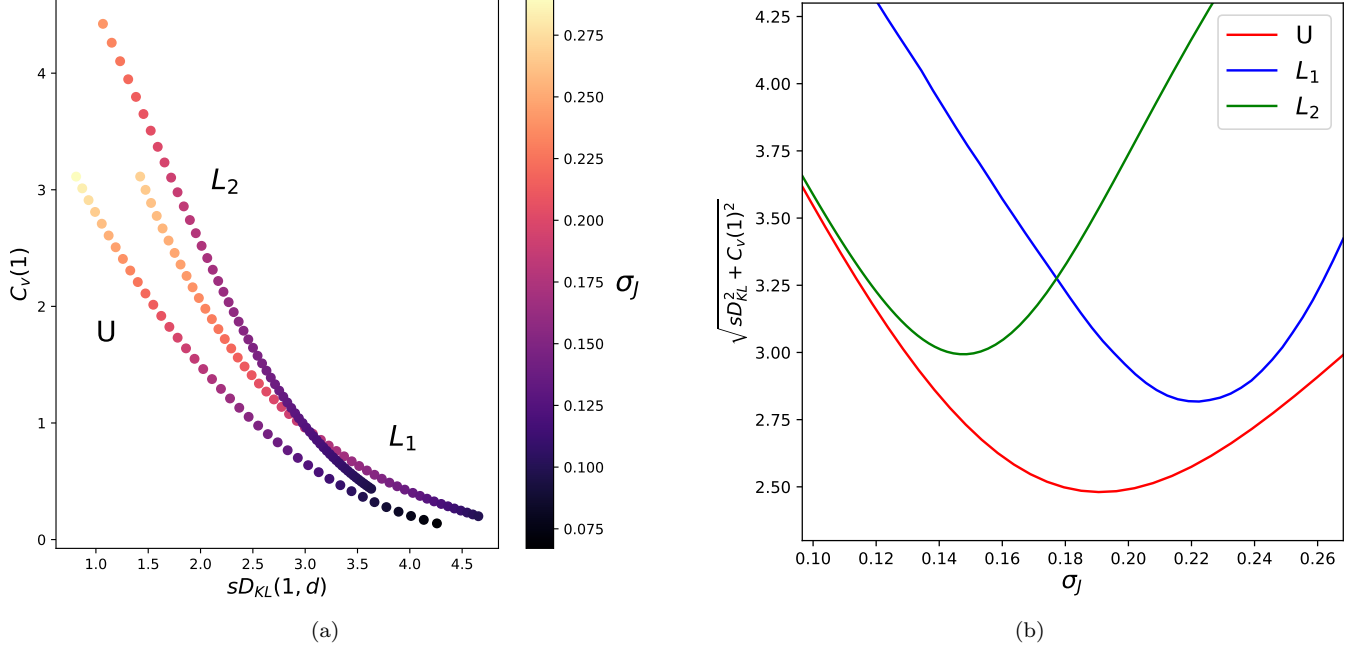


FIG. 6. Comparison of the generalization performance of the unlearning, L_1 and L_2 regularization methods. (a) Symmetric Kullback-Leibler divergence sD_{KL} and specific heat at unitary temperature $C_v(1)$ for different realizations of the standard deviations of the couplings σ_J . (b) Distance from origin of the points in panel (a) as a function of σ_J . Choice of the parameters: $N = 18$, $\beta_d = 0.4$, $a \in \{0.10, 0.21, \dots, 0.50\}$, $\gamma_1 \in \{0.150, 0.155, \dots, 0.400\}$, $\gamma_2 \in \{1.0, 1.1, \dots, 7.0\}$, $\lambda = 0.06$, $\lambda_1 = \lambda_2 = 0.001$.

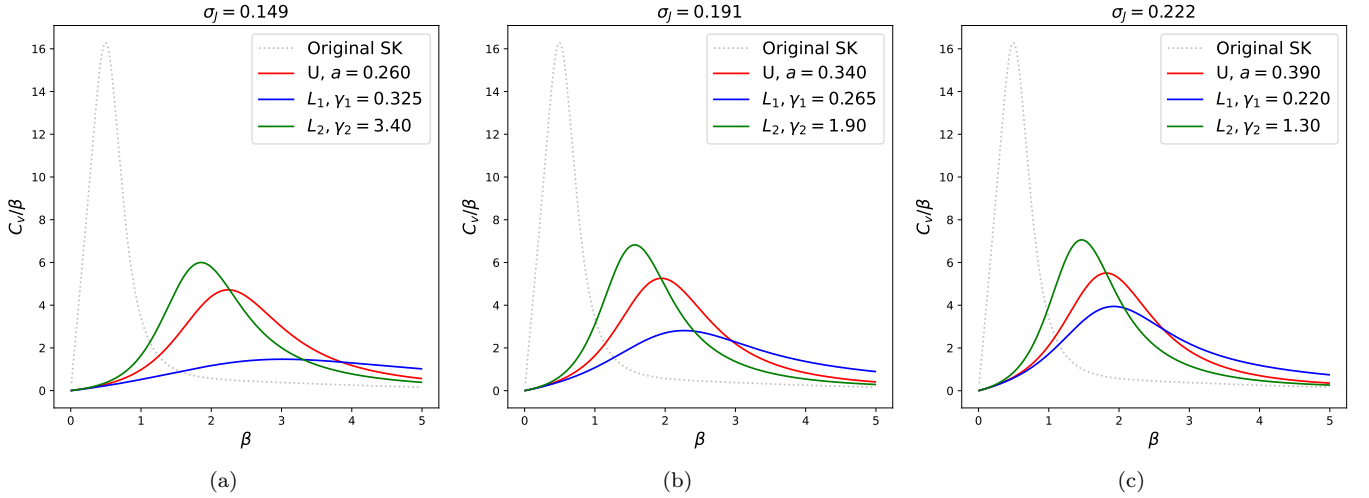


FIG. 7. Specific heat C_v/β versus β for three combinations of (a, γ_1, γ_2) relative to the best generalization performances of the three regularization algorithms. Choice of the parameters: $N = 18$, $\beta_d = 0.4$, $\lambda = 0.06$, $\lambda_1 = 0.001$, $\lambda_2 = 0.001$.

different training steps. Results show, for the first time, that HU can be employed as an inferential tool, due to the beneficial effect of the Hebbian initialization of the couplings. We advance an explanation for its performance that is supported by further numerical evidence. In the limit $a \rightarrow 0$ the updating rules (26) and (27) become

$$\delta J_{ij} = -\lambda \langle S_i S_j \rangle_1, \quad (44)$$

$$\delta h_i = -\lambda \langle S_i \rangle_1. \quad (45)$$

Eq. (44) strongly resembles the traditional HU algorithm of Ref. [8]. By contrast with the original rule, the new regularization samples configurations at $\beta = 1$ instead of stable fixed points of the neural dynamics, and makes use of a thermal average, rather than summing each contribution each time. We will keep dealing with small networks so that, given the initial conditions for the parameters,

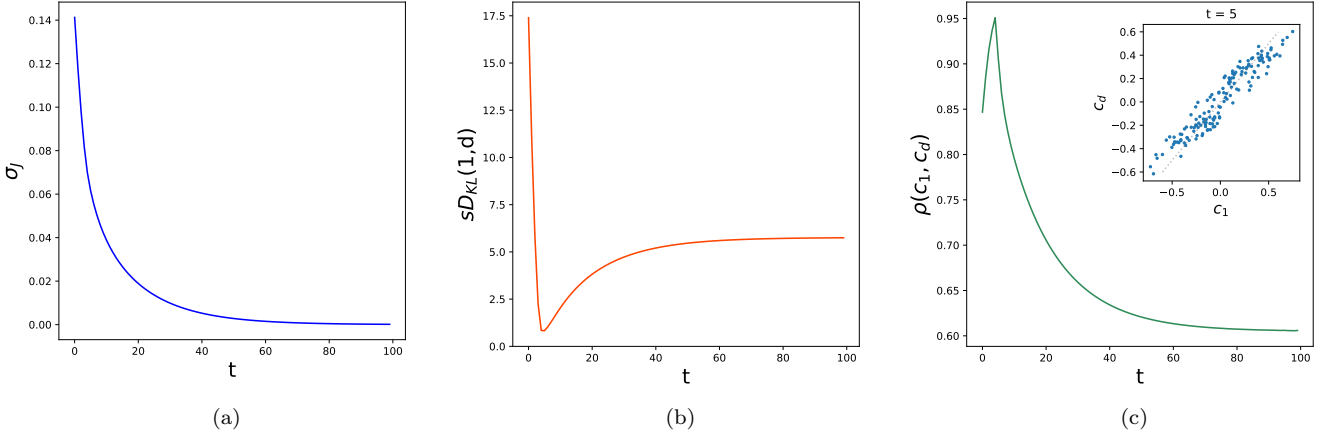


FIG. 8. Three relevant observables to benchmark the inferential performance of the unlearning regularization with $a = 0$: the standard deviation of the couplings σ_J , the Kullback-Leibler divergence between the original SK model and the inferred one at $\beta = 1$, the Pearson coefficient between the data correlation matrix c_d and c_1 , i.e. the correlation matrix for the model at $\beta = 1$. Choice of the parameters: $N = 18$, $\lambda = 0.06$, $\beta_d = 0.4$.

the loss function of the problem can be minimized exactly. As a numerical experiment, we train a BM with $N = 18$ neurons to learn a SK model at $\beta_d = 0.4$. The unlearning regularization is applied with $a = 0$ and the usual initial conditions for the parameters, i.e. $J^{(0)} = c_d$ and $h_i^{(0)} = 0 \forall i$.

Even if training is performed over both the couplings and the fields, according to the rules (44) and (45), the fields \mathbf{h} do not appear in the energy of the original model, hence we will focus exclusively on the evolution of the interactions \mathbf{J} . Fig. 8a displays the standard deviation of the couplings: as we can see the general trend shows an exponential decay of the interactions, as one typically observes in the HU algorithm [9]. The decay to zero is implied by the fact that the fixed point of the gradient descent equations for Eq. (44) corresponds to $c_1 \equiv 0$. Fig. 8b depicts the symmetric Kullback-Leibler divergence between the Gibbs-Boltzmann distribution of the original SK model, from which data were sampled, and the inferred model with $\beta = 1$. The sD_{KL} is high at the beginning, then decreases until reaching a global minimum signaling an optimum in the inferential performance, then it increases again and stabilizes at a plateau. The minimum is sufficiently low to indicate a good statistical consistency between the model and data. The Pearson coefficient between the correlation matrix of the data c_d and the one of the inferred model at unitary temperature c_1 is measured step-by-step in the learning process and reported in fig. 8c: as one can notice, there is a global maximum near the position of the global minimum of the sD_{KL} . The inset in fig. 8c displays the good agreement between the two matrices, the inferred c_1 and c_d , at the position of the peak.

This analysis suggests that the unlearning regularization with $a = 0$ displays two algorithmic regimes: a tran-

sient regime where the model at $\beta = 1$ shows a good statistical agreement with the generating model; another regime where $c_1 \rightarrow 0$, and the total performance deteriorates. The first transient regime is the most important one, because it suggests that HU can be considered as an inferential tool, aside of its associative memory use. We know from section II A that in BM learning data are shown to the model each time-step of the algorithm and this imposes the moment matching. The co-existence of a positive Hebbian term and a negative unlearning one in the traditional BM learning has already been pointed out in Refs. [1, 33]. Let us rewrite the loss of BM learning as the sum of two contributions:

$$\begin{aligned} \mathcal{L} &= \mathcal{L}_{data} + \mathcal{L}_{mod} = \\ &= \sum_{\vec{S}} P_{data}(\vec{S}) \log \left(P_{data}(\vec{S}) \right) - \\ &\quad - \sum_{\vec{S}} P_{data}(\vec{S}) \log \left(P_{mod}(\vec{S}) \right). \end{aligned} \quad (46)$$

The two terms measure, respectively, the opposite of the entropy of the data and the cross-entropy of the model with respect to the data. The variation of each pair of couplings J_{ij} is now given by

$$\nabla_{ij} J = \nabla_{ij}^H J + \nabla_{ij}^U J, \quad (47)$$

where

$$\nabla_{ij}^H J = -\frac{\partial}{\partial J_{ij}} \mathcal{L}_{data} = \langle S_i S_j \rangle_{data}, \quad (48)$$

$$\nabla_{ij}^U J = -\frac{\partial}{\partial J_{ij}} \mathcal{L}_{mod} = -\langle S_i S_j \rangle_{mod}. \quad (49)$$

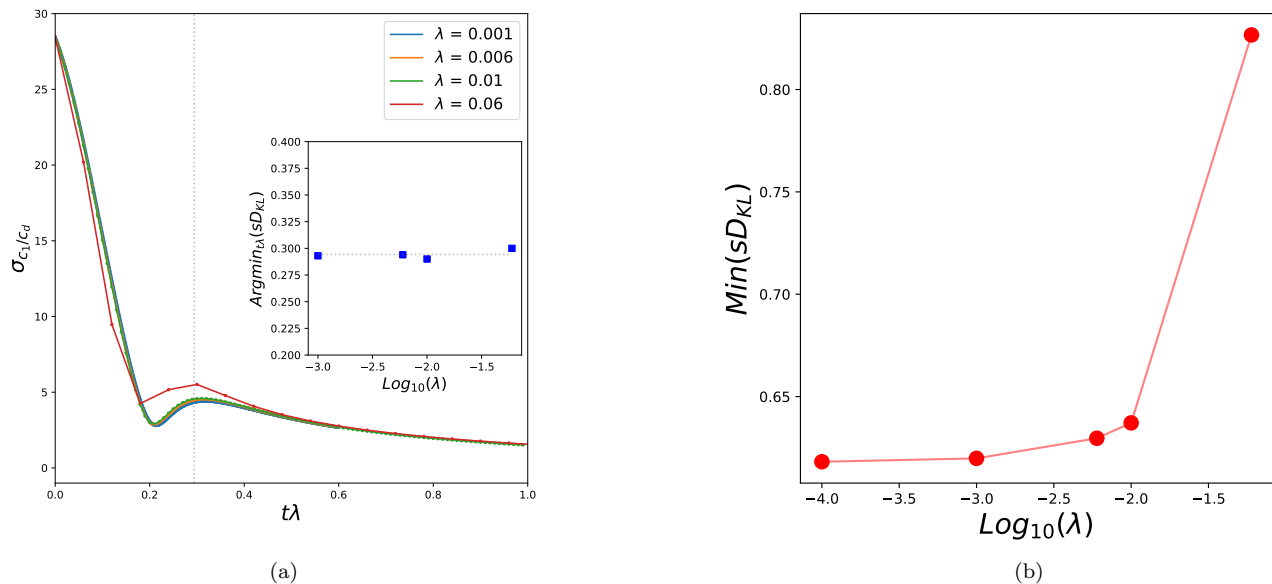


FIG. 9. (a) Standard deviation of the ratio between the elements of c_1 and c_d as a function of the normalized time $t\lambda$; the subplot reports the values of $t\lambda$ associated to global minima of the symmetric Kullback-Leibler divergence (sD_{KL}) between the generating model and the inferred one for different choices of λ ; both the vertical and horizontal gray dotted lines report the mean of the points in the inset. (b) Global minimum of the symmetric Kullback-Leibler divergence between the generating model and the inferred one as a function of λ in log-scale. Choice of the parameters: $N = 18$, $a = 0$, $\beta_d = 0.4$.

While a standard BM can start wherever in the space of the parameters and ends up at the fixed point of eq. (47), in the HU case the update is performed by using only the negative unlearning contribution. Nevertheless, the data have been seen by the model, specifically through the Hebbian choice of the initial conditions. This observation suggests that HU approaches the minimum of the loss function in two steps: firstly minimizing \mathcal{L}_{data} and then progressively descending over \mathcal{L}_{mod} . Even though $\nabla_{ij}^H J$ is constant because it only depends on the training data, $\nabla_{ij}^U J$ must change in time, because it depends on the evolution of the parameters. As a consequence, we can assume that such a two-steps minimization equals the standard BM learning only while

$$|\langle S_i S_j \rangle_{mod}| \gg |\langle S_i S_j \rangle_{data}| \quad (50)$$

for most of the pairs i, j . To test whether this condition holds while training a BM regularized with $a = 0$, and initialized with $\mathbf{J}^{(0)} = \mathbf{c}_d$, we measure the standard deviation of the ratio between the elements of c_1 and c_d as a function of time.

Results are presented in fig. 9a for the usual data-set sampled by a SK model. The standard deviation of the ratio of the elements of the two matrices c_1 and c_d is plotted as a function of $t\lambda$ for different choices of λ . The curves collapse well from λ smaller than $\mathcal{O}(10^{-2})$. The system starts with c_1 generally being much larger than c_d , which satisfies the condition (50). Around $t \sim 0.2\lambda^{-1}$ the curves reach a local minimum, then increase until a

local maximum at $t \sim 0.29\lambda^{-1}$, to start a slow decay right after. Both these two stationary points are located where c_1 and c_d share the same order of magnitude, i.e. where the condition for the two-steps minimization of the loss ceases to hold. However, only the second stationary point is associated to the minimum of the sD_{KL} between the original SK and the model, as reported in the inset of fig. 9a. Moreover, fig. 9b reports the values assumed by sD_{KL} at its global minimum for various choices of λ . As one can notice, the generalization of the model increases when λ is small: we can imagine that the smaller is λ the stronger is the effect of the initial overshooting at minimizing \mathcal{L}_{data} .

Different parameter initializations can now be compared. Specifically, we run the standard BM learning (i.e. the unlearning regularization with $a = 1$) after a Hebbian, random, and all-to-zero initialization of the couplings. The Hebbian and the random initializations have the same initial standard deviation of the couplings σ_J . At this stage we measure the evolution in time of the standard deviation of the ratio c_1/c_d and the value of the loss. In addition to these two quantities, we introduce another observable that quantifies the degree of alignment of the gradient

$$\vec{\nabla} J(t) = -\vec{\nabla} \mathcal{L}(t) \quad (51)$$

to the direction connecting the initial state of the couplings, i.e. $\mathbf{J}^{(0)}$, and the convergence state $\mathbf{J}_d = \beta_d \mathbf{J}^{SK}$.

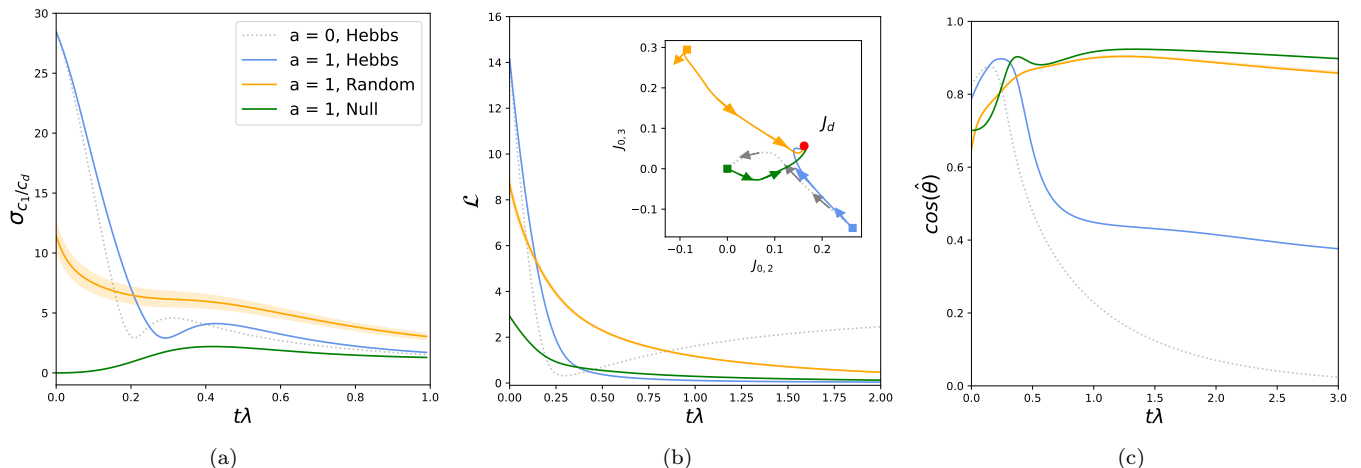


FIG. 10. Confronting different initializations of the parameters. (a) Standard deviation of the ratio between the elements of c_1 and c_d as a function of the normalized time $t\lambda$ in a standard BM learning scenario (i.e. unlearning regularization with $a = 1$). (b) Loss function \mathcal{L} as a function of the normalized time $t\lambda$ in a standard BM learning scenario. (c) Cosine of the angle between the gradient of \mathbf{J} and the direction connecting the initial state of the parameters $\mathbf{J}^{(0)}$ and the model to be inferred \mathbf{J}_d . The curve for the unlearning regularization with $a = 0$ is indicated in all panels for comparison. The curve relative to the random initialization is averaged over fifteen starting matrices and the halo represents the standard deviation of the measures. Choice of the parameters: $N = 18$, $\beta_d = 0.4$, $\lambda = 0.01$.

Such quantity is defined as

$$\cos(\hat{\theta}) = \frac{\vec{\nabla} J \cdot (\vec{J}_d - \vec{J}^{(0)})}{|\vec{\nabla} J| |\vec{J}_d - \vec{J}^{(0)}|}. \quad (52)$$

The evolution of these observables are reported in fig. 10. Note that, for the random initialization, measures are averaged over fifteen realizations of the initial matrix. As one can observe from fig. 10a, the highest ratio c_1/c_d is obtained by the Hebbian initialization; the random initialization also begins with the elements of c_1 being on average larger than the empirical data correlations. Yet, as one can see from fig. 10b, the loss decays generally faster in the Hebbian case, with respect to the random case. Figure 10c allows to interpret the behavior of the learning dynamics in terms of the gradient descent: the Hebbian initialization points the gradient $\vec{\nabla} J$ towards the minimum of the loss, located in \mathbf{J}_d ; on the other hand, the random initialization does not start well in its descent, and progressively adjusts the trajectory. The wrong start of training after random initialization can be also visualized in the inset of fig. 10b, displaying a projection of the trajectory over the first two components of the \mathbf{J} matrix, with arrows indicating the direction of the gradient descent. Only one experiment is reported for the random initialization since the others showed very similar behavior. Conversely, when the system learns from zero initial couplings, both the positive and negative contributions to the learning appear to be small and comparable in value, which implies that the implementation of pure unlearning is ineffective in this case; the descent of the loss is slower with respect to the Hebbian initialization; the trajectory is already sufficiently pointing to the bot-

tom of the landscape, and progressively adjusts itself.

We conclude by another important remark. The unlearning trajectory and the standard BM learning look very similar in the first stage of training, in terms of the gradient descent, as predicted by Eq. (50). After a certain amount of iterations that we have identified above, the unlearning trajectory deviates towards $\mathbf{J} = \mathbf{0}$, while the BM finally converges to the final target. The abrupt change of direction that is visible from both the two-dimensional projection of the trajectory and the evolution of the gradient might be related to the choice of the data-set. We have thus showed that, when the network is initialized in the Hebbian fashion, the dominant contribution to the BM learning is the unlearning one, and the gradient of \mathbf{J} points towards the minimum of the loss function. Hence we showed that the HU algorithm works as well as an inferential device than as a training procedure for associative memory models.

VII. CONCLUSIONS

In this study we have shown that:

- In the context of Boltzmann Machines, and specifically for what concerns the generalization performance of the inferred network, the standard L_1 and L_2 regularization techniques are outperformed by the unlearning regularization.
- A particular case of the unlearning regularization (i.e. for a vanishing parameter a) reproduces a thermally averaged Hebbian Unlearning rule, that shows good inferential capabilities when initialized

in the standard Hebbian fashion. Hebbian Unlearning can be interpreted as a two-steps Boltzmann-Machine learning and it is well reproduced by a L_2 regularization with a high regularization rate. By contrast with the instance of $a > 0$, where the algorithm runs until convergence of the gradient descent equations, this particular case shows the necessity of early-stopping the training procedure after a specific amount of iterations where the performance reaches its optimum.

The goal of this article was thus to show the effectiveness of unlearning as a form of regularization in Boltzmann Machines. For this purpose, we have used small networks that allowed to compute all quantities without error by exact enumeration. Precisely, the ground-truth distribution was defined by one of two models, either the Curie-Weiss or the Sherrington-Kirkpatrick models, which are known to show a phase transition at a critical temperature. As a result, we could not only test the proximity of the inferred model to the original one, but also the susceptibility of the network under variations of the parameters, by comparing the trend of the specific heat of the ground truth model with respect to the inverse temperature, with the trend obtained after inference with regularization. We conclude that the two main components that define the generalization of the model, i.e. its consistency with the ground-truth distribution and its stability under rescaling of the parameters, are enhanced by the unlearning regularization.

In a more realistic scenario with the model fitting real data, the ground-truth distribution is not known a-priori. As a consequence one cannot benchmark the generalization performance of the model by evaluating its distance from the real data distribution, as we did in conditions of perfect sampling. A cross-validation procedure must be implemented in analogy to what is done with other types of regularizations. We thus propose to divide the real data-set in two different parts: a *training* set, that is used to train the model with a certain choice of the control parameter a ; a *testing* set, with an empirical data distribution, that is now compared to the inferred model at unitary temperature with the empirical distribution of the data because we know, from our analysis, that this model is the closest one to the ground-truth. The training procedure is repeated for several choices of a , and the value of the variable that gives the highest resemblance of the model with the statistics of the testing set, as well as the lowest $C_v(1)$ (in analogy to the analysis reported in fig. 6b), is adopted as a winning choice for the hyperparameter. A test on a real data-set is a straightforward proceeding of our study.

Moreover we analyzed the particular limit of the regularization that gives as learning rules the ones expressed in equations (44) and (45). The resulting procedure

strongly resembles the traditional Hebbian Unlearning routine, but with a thermal two-point correlation computed at $\beta = 1$ replacing that computed on the zero-temperature fixed points of the dynamics. Previous work [12] support the fact that the associative memory performance of such a *thermal* unlearning does not deviate much from the original rule. As a new contribution to the characterization of unlearning, we tested its inferential power, i.e. the capability of learning the original model. So far, to the best of our knowledge, the unlearning algorithm was exclusively tested in an associative memory framework, where data are actually patterns, that are sub-dominant in number with respect to the entire set of possible configurations. Our results show a good generalization performance of the algorithm. The explanation for this success relies on the choice of the initialization of the parameters. A Hebbian initialization of the network has two implications. First, the contribution to the gradient of the loss deriving from the data (i.e. the positive *Hebbian* contribution in the Boltzmann Machine learning in eq. (46)) is much smaller than the contribution deriving from the cross-entropy of the model given the data (i.e. the negative *unlearning* contribution in the Boltzmann Machine learning). This condition holds until an optimal amount of iterations that can be estimated from the numerical simulations. Second, we showed that a Hebbian initialization of the couplings points the gradient of the parameters towards the correct direction, i.e. the one of the ground-truth of the inferential problem, at variance with other kinds of parameter initialization.

We conclude that Boltzmann Machine learning can be performed in two steps: an initial overshooting along the *direction of the data* and then a gradual adjustment along the *direction of the model* with increments being updated at each step of the algorithm. The effectiveness of a two-step training for a Boltzmann Machine encourages a biological interpretation of this kind of training, in agreement with the hypothesis that synapses in the brain could be fine tuned through the alternation of daily online experience and offline sleep [34, 35]. Such a conjecture is inspiring members of the A.I. community in the development of training procedures for deep neural networks that might substitute the slow and non-biological back-propagation techniques [33, 36]. These observations, together with the importance of the Hebbian initialization of the network, appear to be consistent with previous results in literature concerning the unlearning algorithm and its implementation in associative memory modeling [9, 10].

ACKNOWLEDGMENTS

We thank Marco Benedetti, Matteo Bisardi, Simone Ciarella, Sabrina Cotogno, Gabrielle Girardeau, Enzo Marinari, Felix Cosmin Mocanu, Giancarlo Ruocco and Jeanne Trinquier for many useful discussions.

-
- [1] G. Hinton and T.J. Sejnowski. *Unsupervised Learning: Foundations of Neural Computation*. The MIT Press, 1999.
- [2] G. Hinton. Boltzmann machine. *Scholarpedia*, 2(5):1668, 2007.
- [3] S. Cocco, R. Monasson, and F. Zamponi. *From Statistical Physics to Data-driven Modelling: With Applications to Quantitative Biology*. Oxford University Press, 2022.
- [4] T. Jebara. *Machine Learning: Discriminative and Generative*. Springer Science & Business Media, 2012.
- [5] William P Russ, Matteo Figliuzzi, Christian Stocker, Pierre Barrat-Charlaix, Michael Socolich, Peter Kast, Donald Hilvert, Remi Monasson, Simona Cocco, Martin Weigt, et al. An evolution-based model for designing chorismate mutase enzymes. *Science*, 369(6502):440–445, 2020.
- [6] T. Mora and W. Bialek. Are Biological Systems Poised at Criticality? *Journal of Statistical Physics*, 144(2):268–302, 2011.
- [7] I. Mastromatteo and M. Marsili. On the criticality of inferred models. *Journal of Statistical Mechanics: Theory and Experiment*, 2011(10):P10012, 2011.
- [8] J.J. Hopfield, D.I. Feinstein, and R.G. Palmer. ‘Unlearning’ has a stabilizing effect in collective memories. *Nature*, 304(5922):158, 1983.
- [9] J.L. Van Hemmen, L.B. Ioffe, R. Kühn, and M. Vaas. Increasing the efficiency of a neural network through unlearning. *Physica A: Statistical Mechanics and its Applications*, 163(1):386, 1990.
- [10] M. Benedetti, E. Ventura, E. Marinari, G. Ruocco, and F. Zamponi. Supervised perceptron learning vs unsupervised Hebbian unlearning: Approaching optimal memory retrieval in Hopfield-like networks. *The Journal of Chemical Physics*, 156(10):104107, 2022.
- [11] M. Benedetti and E. Ventura. Training neural networks with structured noise improves classification and generalization. *arXiv:2302.13417*, 2023.
- [12] K. Nokura. Paramagnetic unlearning in neural network models. *Physical Review E*, 54(5):5571, 1996.
- [13] C. M. Bishop. *Neural Networks for Pattern Recognition*. Clarendon Press, 1995.
- [14] S. Cocco, S. Leibler, and R. Monasson. Neuronal couplings between retinal ganglion cells inferred by efficient inverse statistical physics methods. *Proceedings of the National Academy of Sciences*, 106(33):14058–14062, 2009.
- [15] E. Schneidman, M. Berry, R. Segev, and W. Bialek. Weak pairwise correlations imply strongly correlated network states in a neural population. *Nature*, 440(7087):1007–1012, 2006.
- [16] F. Morcos, A. Pagnani, B. Lunt, A. Bertolino, D.S. Marks, C. Sander, R. Zecchina, J.N. Onuchic, T. Hwa, and M. Weigt. Direct-coupling analysis of residue coevolution captures native contacts across many protein families. *Proceedings of the National Academy of Sciences*, 108(49):E1293–E1301, 2011.
- [17] X. Chen, M. Winiarski, A. Puścian, E. Knapska, T. Mora, and A. M. Walczak. Modelling collective behavior in groups of mice housed under semi-naturalistic conditions. *bioRxiv 2023.07.26.550619*, 2023.
- [18] K. Sims. Evolving virtual creatures. In *Proceedings of the 21st annual conference on Computer graphics and interactive techniques*, 1994.
- [19] A. Brock, J. Donahue, and K. Simonyan. Large Scale GAN Training for High Fidelity Natural Image Synthesis. *arXiv:1809.11096*, 2019.
- [20] P. Kawthekar. *Evaluating Generative Models for Text Generation*. PhD thesis, Stanford University, 2017.
- [21] J. Sohl-Dickstein, E. Weiss, N. Maheswaranathan, and S. Ganguli. Deep Unsupervised Learning using Nonequilibrium Thermodynamics. In *Proceedings of the 32nd International Conference on Machine Learning*, pages 2256–2265. PMLR, 2015.
- [22] M. I. Jordan and T. J. Sejnowski. *Graphical Models: Foundations of Neural Computation*. MIT Press, 2001.
- [23] G. Tkačik, T. Mora, O. Marre, D. Amodei, S. E. Palmer, M. J. Berry, and W. Bialek. Thermodynamics and signatures of criticality in a network of neurons. *Proceedings of the National Academy of Sciences*, 112(37):11508–11513, 2015.
- [24] L. D. Landau and E. M. Lifshitz. *Statistical Physics*. Elsevier Science, 1980.
- [25] P. Barrat-Charlaix, A. P. Muntoni, K. Shimagaki, M. Weigt, and F. Zamponi. Sparse generative modeling via parameter reduction of Boltzmann machines: Application to protein-sequence families. *Physical Review E*, 104(2):024407, 2021.
- [26] F. Crick and G. Mitchison. The function of dream sleep. *Nature*, 304(5922):111, 1983.
- [27] J.L. Van Hemmen and N. Klemmer. Unlearning and Its Relevance to REM Sleep: Decorrelating Correlated Data. In J.G. Taylor, C.L.T. Mannion, J.G. Taylor, E.R. Caianiello, R.M.J. Cotterill, and J.W. Clark, editors, *Neural Network Dynamics*, page 30. Springer London, London, 1992.
- [28] S. Wimbauer, N. Klemmer, and J.L. van Hemmen. Universality of unlearning. *Neural Networks*, 7(2):261, 1994.
- [29] D. Kleinfeld and D. Pendergraft. Unlearning increases the storage capacity of content addressable memories. *Biophysical Journal*, 51:47, 1987.
- [30] E. Gardner. Structure of metastable states in the Hopfield model. *Journal of Physics A: Mathematical and General*, 19(16):L1047, 1986.
- [31] D.J. Amit. *Modeling Brain Function*. Cambridge University Press, 1989.
- [32] D. Sherrington and S. Kirkpatrick. Solvable Model of a Spin-Glass. *Physical Review Letters*, 35(26):1792, 1975.
- [33] G. Hinton. The Forward-Forward Algorithm: Some Preliminary Investigations. *arXiv:2212.13345*, 2022.
- [34] J. Payne and L. Nadel. Sleep, dreams, and memory consolidation: The role of the stress hormone cortisol. *Learning and Memory*, 11(6):671, 2019.
- [35] G. Girardeau and V. Lopes-dos Santos. Brain neural patterns and the memory function of sleep. *Science*, 374(6567):560–564, 2021.
- [36] B. Scellier and Y. Bengio. Equilibrium propagation: Bridging the gap between energy-based models and backpropagation. *Frontiers in Computational Neuroscience*, 11(24), 2017.